Dynamics and Energetics of the Self-Assembly of a Hydrophobically Modified Polyelectrolyte: Naphthalene-Labeled Poly(Acrylic Acid)

ARTICLE *in* THE JOURNAL OF PHYSICAL CHEMISTRY B · JULY 2005

Impact Factor: 3.3 · DOI: 10.1021/jp050236v · Source: PubMed

5 AUTHORS, INCLUDING:

Telma Costa
University of Coimbra
30 PUBLICATIONS **307** CITATIONS
SEE PROFILE

Bjorn Lindman
Lund University
574 PUBLICATIONS **19,796** CITATIONS
SEE PROFILE

Karin Schillén
Lund University
80 PUBLICATIONS **2,865** CITATIONS
SEE PROFILE

J. Sérgio Seixas de Melo
University of Coimbra
161 PUBLICATIONS **3,599** CITATIONS
SEE PROFILE

Dynamics and Energetics of the Self-Assembly of a Hydrophobically Modified Polyelectrolyte: Naphthalene-Labeled Poly(Acrylic Acid)

Telma Costa,[†] Maria da G. Miguel,[†] Björn Lindman,[†,‡] Karin Schillén,[‡] and J. Sérgio Seixas de Melo*,[†]

Chemistry Department, University of Coimbra, 3004-535 Coimbra, Portugal, and Physical Chemistry 1, Center for Chemistry and Chemical Engineering, Lund University, Lund, Sweden

Received: January 13, 2005; In Final Form: April 1, 2005

Steady-state and time-resolved fluorescence studies were performed on aqueous solutions of poly(acrylic acid) hydrophobically modified with two very different levels of naphthalene (Np). It is demonstrated that unique information on association phenomena involving hydrophobe-modifed polymers can be obtained from an extended fluorescence study by using data for a less-modified polymer as a reference. For the more highly modified polymer, the presence of excited-state (as well as ground-state) dimers in addition to monomer emission due to locally excited naphthalene gives evidence for hydrophobic association between naphthalene groups. This association becomes, as expected, much less important at higher pH due to the electrostatic repulsion between different chain segments. However, it is noted that even at high pH there is a significant self-association. The coexistence of static and dynamic quenching phenomena of the Np monomer label was also revealed in the time-resolved fluorescence data. The data are compatible with the existence of two types of monomers and one excimer and suggest that the essential contribution to the monomer emission comes from isolated chromophores, whereas excimer formation arises from both a dynamic route (excited Np chromophores able to produce a dynamic excimer) and a static route (excitation of ground-state Np dimers). At room temperature, the dissociative reaction, excimer-to-monomer, can be neglected, and thus the rate constant for excimer formation and decay could be obtained with and without considering the influence of preformed dimers. Temperature has shown to induce different behavior in the polymer photophysics. In the case of the less-labeled polymer, the decays were found to be single-exponential with the fluorescence lifetime decreasing with increasing temperature. From the temperature dependence of the steady-state fluorescence data, the activation energy for excimer formation and the binding energy of the excimer were evaluated at different pH values, through the Stevens−Ban-type plots of the excimer-to-monomer intensity ratio. With the time-resolved data, measured in the temperature range of 5−60 °C, it was possible to extract the intrinsic activation energies for excimer formation. The thermodynamic driving force for the intrapolymeric association was found to be dependent on a balance between hydrophobic and electrostatic interactions, which are dependent on the pH, temperature, and hydrophobic content of the polymer.

Introduction

The study and use of polyelectrolytes are of major importance in the colloid domain, the classical example of their practical use being the control of the stability of colloidal dispersions, for example, in paper-making to flocculate cellulose fibers.[1] In the case of hydrophobically modified water-soluble polymers, those that have been developed during the last two decades can now be found in all modern water-based paints. Associating polymers have important applications for surface modification, structuring, and, in particular, rheology control.[2] Rheological properties of associating polymer solutions are to a first approximation determined by the number of cross-links and their lifetimes. For the understanding of such systems and thus to allow a more systematic development of "thickeners" for many applications, a direct monitoring of the lifetimes and how they are affected by various chemical and physical parameters is fundamental. It is, therefore, of relevance to study the dynamics of such systems on a molecular level. Time-resolved complemented with steady-state fluorescence spectroscopy then appears as a technique of choice since by choosing the adequate time resolution the monitoring of molecular events can be done. No probe needs to be added since the fluorescent hydrophobic groups give rise to the desired rheological effects; important commercial thickeners in fact contain aromatic fluorescent groups. Of interest is also to study the effect induced by a change of the hydrophobic group and the degree of hydrophobic modification of the water-soluble polymer.

Poly(acrylic acid) (PAA) is an example of a polymer of particular interest in colloidal systems. In fact, in addition to the particular role displayed by being a charged polymer (except at low pH), the aqueous solubility of this polyelectrolyte can further influence the electrostatic forces between colloidal particles. By hydrophobically modifying the polymer, with alkyl or aromatic groups, which may be fluorescent such as naphthalene (Np) or pyrene chromophores, a balance between electrostatic forces and hydrophobic interactions can be induced.[3−5] The introduction of the fluorescent probe allows the polymer to be followed by luminescent techniques at very

* Author to whom correspondence should be addressed. Fax: 351 239 827703. E-mail: sseixas@ci.uc.pt.
[†] University of Coimbra.
[‡] Lund University.

10.1021/jp050236v CCC: $30.25
Published on Web 05/21/2005

low concentrations, thus permitting a conformational study of the isolated polymer. As a consequence, the measurements presented here were all performed in the dilute concentration regime, i.e., $c < C^*$.[1,2]

Due to the ionizing carboxyl groups (COOH) in the PAA backbone, it is possible to induce different polymer chain configurations by varying the hydrogen ion concentration of the media.[3,4] In addition, the presence of hydrophobic groups, randomly introduced into the chain, provides hydrophobic associations that compete with the electrostatic repulsions resulting from the ionized carboxyl groups. In view of these competing processes, the polymer chain can undergo conformational changes, which can be probed by the hydrophobic aromatic units. Due to these hydrophobic modifiers, the PAA molecules can never be in the extreme stiff-rod configuration.[1] In fact, even when the PAA backbone structure is completely ionized and thus electrostatic repulsions would lead the polymer chain to adopt a more extended conformation, the presence of locally neighboring hydrophobes will lead to association and consequently to the local coiling of a polymer segment. In the present work, it will be shown that PAA modified with various levels of naphthalene, PAAMeNp34 (high level of Np) and PAAMeNp200 (low level of Np), can induce different configurational random coil states.

In the situation where $c < C^*$,[1,2] applicable in the present case, interpolymer interactions are absent, and when discussing the various levels of polymer chain conformation, only interactions within the single chain will be considered. Consequently, the hydrophobic ground-state associations between the Np groups, which can be followed by the appearance of a new emissive band, are only due to intramolecular and not intermolecular naphthalene association. Intramolecular excimer formation is frequently used to study polymer interactions and conformational changes. Common excimer-forming probes are carbazole,[6−8] pyrene,[6] and naphthalene.[6,9] Unlike their fluorescent probe units in homogeneous solution, grafted polymers frequently show complex luminescence decay behavior, displaying multiexponential decay laws as the rule and not the exception. Consequently, fluorescence techniques and in particular monomer−excimer time-resolved emission are useful tools to study polymer dynamics. The fingerprint for excimer formation is the observation of an additional structureless band in the emission spectra. Excimer formation kinetics in fluid solutions are explicable in terms of the Birks[10] scheme, where the encounter of an excited monomer (M*) with a nonexcited monomer (M) kinetically leads to the formation of an excimer (E*) with a rate constant k_a. This rate constant may be concentration-dependent (with respect to the monomer) if the process is intermolecular (k_a[M]) but not if the process is intramolecular. Exceptions to this case are, for example, the randomly labeled polymers,[3,4,11] exemplified by the studied systems where the percentage of grafted naphthalene into the polymer determines the level of excimer formed. The formed excimer either dissociates to give M* and M with a rate constant k_d or it deactivates to the ground state (k_E) giving rise to two monomer units. Additionally, in this Birks' kinetic scheme the excited monomer can also be directly deactivated to the ground state with a rate constant k_M. Several issues intrigued workers involved in the observation of intramolecular excimer emission in polymers, in particular certain puzzling features observed in the decays of some carbazole-, pyrene-, and naphthalene-based polymers.[12] In the mid-1960s, this led to the general idea that the application of Birks' formalism to polymer photophysics had to be modified. Later on, in the 1980s, a revision of the model of monomer−excimer kinetics for polymers was proposed.[13] It was then suggested that, in principle, Birks' formalism was not applicable to fluorescent polymers. In the large majority of the initially proposed models, three species were involved, one monomer and two excimers[8,14,15] or two monomers and one excimer.[13,16,17] In one study of particular interest, Holden et al.[13] proposed that one monomer species is "isolated" from the excimer formation scheme, thus showing an emission characteristic of an unquenched chromophore. More recently, a series of poly(ethylene glycol)s with a central chain connecting two pyrene chromophores and with these flanked by end chains of different lengths have shown that the classic Birks' kinetic scheme has to be extended with a third component (isolated unquenched pyrene monomer lifetime).[18]

When polymer properties are studied, fluorescence emission contains in itself a dynamic property since the absorption of a photon by the fluorophore in the chain produces, immediately and locally, a perturbation in the backbone chain, which in a solution medium is moving on the same time scale as the excited-state lifetime (τ_M). In a randomly labeled polymer with aromatic moieties, such as the presently studied polymers, there are regions within the polymer richer in the fluorophore coexisting with others where the fluorophore is isolated (i.e., it has no neighboring chromophore capable of inducing excimer formation). If the macromolecule is completely immobilized, a situation not very probable in solution, then the relative intensity of the excimer-to-monomer bands (I_E/I_M) will only depend on the quantity of sites rich in the fluorophore, or excimer-forming sites (EFS).[19] If conformational equilibria within the polymer are allowed to occur, then this I_E/I_M ratio will vary, thus giving information concerning the conformational state of the polymer. Therefore, in solution media, the analysis of the dependence of the steady-state fluorescence ratio I_E/I_M on temperature together with time-resolved measurements of monomer and excimer decays can provide kinetic and thermodynamic parameters, allowing interpretation of the macromolecule behavior. These have been the objectives of the present investigation.

Although the nature of the excimer formation process in the current work is intramolecular, the random labeling of the polymer leads to different interchromophoric distances, and as a consequence the rate constant for excimer formation will be dependent on the labeling degree (hydrophobe concentration in the chain). This means that there is a fluorophore concentration dependence for a given polymer but not a variation with the concentration of polymer itself, which parallels the above-mentioned situation of intermolecular excimer formation; however, in this case, k_a indirectly depends on the concentration of naphthalene grafted onto the polymer chain, $k_a = k_a'$[Np], where [Np] reflects the number of Np units per PAA unit, which is higher for the more highly labeled polymer (PAAMeNp34, see below) than it is for the less-labeled PAAMeNp polymer (PAAMeNp200). In the limit, as is the case for the less-labeled polymer, there is no excimer formation since $k_M \gg k_a$. It is the distribution of excimer-forming sites that can lead to a distribution of the rate constants for excimer formation that led Duhamel and co-workers to develop the so-called "blob model".[20,21] However, we have shown[3] and will confirm in the present work that the alternative treatment, allowing discrete (with little degree of error) excimer-forming rate contants, gives additional and alternative information to that obtained with the blob model.

The present work aims to extend previous studies made with analogous[3,5,22] and identical[4,11] randomly modified PAA polymers. Particular emphasis will be put on the effect of the variation of the hydrogen ion concentration of the media and

SCHEME 1

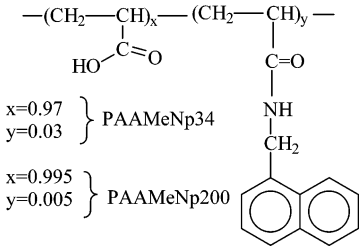

its influence on the polymer photophysics. A kinetic scheme accounting for the coexistence of isolated and excimer-forming Np chromophores will be presented, and the pertinent differential equations will be solved to extract the rate constants for excimer formation (k_a) and deactivation (k_E). The absence of competitive thermal reversibility excimer-to-monomer, at room temperature, greatly simplifies the differential kinetic equations. The presence of ground-state preformed dimers (GSDs) will also be considered in the determination of the true excimer formation ($k_a(\alpha)$) and deactivation ($k_E(\alpha)$) rate constants.

Experimental Section

A 25% aqueous solution of PAA with nominal molecular weight of 150 000 g/mol was purchased from Wako Chemicals, Japan. Before being labeled with 1-naphthyl methylamine, the solution was freeze-dried to give solid PAA, which was used in the postmodification step. The synthesis followed the same route as previously described.[3,4,11,22] Two naphthyl (Np)-labeled PAA samples were prepared, one with a higher and one with a lower amount of naphthalene groups. All chemicals used in the syntheses were of reagent grade. 1-Naphthylmethylaminehydrochloride, 1,3-dicyclohexylcarbodiimide, and anhydrous 1-methylpyrrolidone were received from Aldrich Chemicals. Spectrum Medical Industries supplied the dialysis membranes with a molecular weight cutoff of 12 000−14 000 g/mol. The amounts of naphthalene were determined both by UV absorption measurements using 1-naphthylmethylamine hydrochloride as a model compound and by ^{1}H NMR measurements in deuterium oxide. The naphthalene content of the more highly labeled PAA polymer was determined to be $[Np]_{UV} = 2.96$ mol % (4.1×10^{-4} mol/g polymer) and $[Np]_{NMR} = 3.25$ mol % (4.5×10^{-4} mol/g polymer). It corresponds to 1 chromophore per 34 acrylic acid unimer units. This sample is denoted PAAMeNp34; see Scheme 1. The naphthalene content was obtained in a similar fashion for the second labeled PAA polymer, and it corresponds to 1 Np unit per 200 acrylic acid unimer units. This sample is denoted PAAMeNp200; see Scheme 1.

The solvents used for the polymer solutions were of spectroscopic or equivalent grade. Water was twice distilled and passed through a Millipore apparatus. The measured pH values were obtained with a Crison Micro-pH 2000, and adjustments of the hydrogen ion concentration of the solutions were made with dilute HCl (or perchloric acid) and NaOH solutions. The chromophore concentration of the aqueous PAAMeNp200 solutions ranged from 1×10^{-5} to 1×10^{-6} M. Prior to experiments, solutions were deoxygenated by bubbling with N_2 or Ar gas and sealed.[23] This procedure was utilized for both time-resolved and steady-state experiments. The polymer concentration in the different solutions was 0.05 g/L, which for this molecular weight is well below the critical value for coil overlap, c^*, and intermolecular chain contacts are therefore improbable in homogeneous solutions. In fact, as stated elsewhere, a concentration of 0.05 g/L is still far below the overlap concentration ($c^* \cong 1/[\eta]$, where $[\eta]$ stands for the intrinsic viscosity of the polymer[24]) of the unlabeled PAA, which was found to be approximately 10 g/L in water at pH $\cong$ 3.[4]

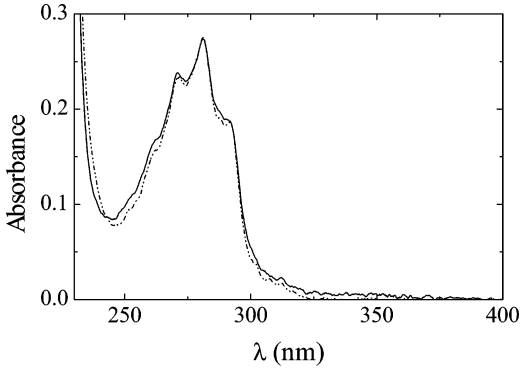

Figure 1. Absorption spectra for PAAMeNp34 (—) and PAAMeNp200 (···) obtained at $T = 293$ K and for pH = 5.7.

Absorption and fluorescence spectra were recorded on Shimadzu UV-2100, Olis-Cary 14, and Jobin-Ivon SPEX Fluorog 3-22 spectrometers, respectively. All of the fluorescence spectra were corrected for the wavelength response of the system. The low optical density of the samples used prevents self-absorption or inner filter effects.

Fluorescence decays were measured using a home-built time-correlated single-photon timing apparatus previously described.[25,26] In short, it consists of a D_2 or N_2 gas-filled IBH 5000 coaxial flashlamp as an excitation source, Jobin-Ivon monochromator, Philips XP2020Q photomultiplier, and Canberra Instruments time-to-amplitude converter and multichannel analyzer. Alternate measurements (1000 counts per cycle at the maximum) of the pulse profile at 285 nm (or 295 nm) and the sample emission were performed until $4-10 \times 10^3$ counts at the maximum were reached. The fluorescence decays were analyzed with a Pentium 500 PC, running LINUX Red Hat as the operating system, using the method of modulating functions of Striker with automatic correction for the photomultiplier "wavelength shift".[27]

Temperature control was achieved using a home-built system based on cooled nitrogen and electric heating, which is automatically controlled by the difference between the input temperature value and the sample real temperature, determined with a PT100 thermometer.

The results from steady-state fluorescence experiments are presented as emission and excitation spectra but often also in terms of the ratios I_E/I_M (ratio of the excimer-to-monomer bands), which result from the decomposed area under the monomer and excimer bands. The general procedure to obtain the I_E/I_M ratio values consisted of matching the emission spectra of the less-labeled polymer (PAAMeNp200), where only the monomer band is displayed, with the monomer band of the PAAMeNp34 polymer. The resulting subtracted spectrum is the excimer emission band.

Results and Discussion

Dynamics. *Absorption Spectra.* The absorption spectra of the PAAMeNp34 and PAAMeNp200 polymers are shown in Figure 1. All measurements in this study were performed at a low concentration of the polymers (0.05 g/L) to avoid intermolecular interactions in solution. The spectra of the polymers strongly resemble the spectrum of naphthalene itself with a characteristic absorption band with the $S_0 \rightarrow S_2[^1L_a(^1B_{3u})]$ and $S_0 \rightarrow S_1[^1L_b(^1B_{2u})]$ transitions at, respectively, the absorption maximum ($\sim$280 nm) and at the red edge of the spectra ($\sim$310 nm).[28] In

TABLE 1: Spectroscopic Parameters Obtained from the Absorption and Fluorescence Excitation Spectra for PAAMeNp34 at Different pH Values[a]

pH	2.67 (±0.12)	3.20 (±0.11)	6.45 (±0.36)	8.46 (±0.33)	11.28 (±0.25)
$\Delta\lambda_1$[b]/nm (±0.3)	1.6	0.8	0.73	0.40	0.20
$\Delta\lambda_2$[c]/nm (±0.3)	1.4	1.2	0.5	0.45	0.2

[a] Also presented are the associated error margins for all of the parameters (resulting from four to five independent measurements). [b] The $\Delta\lambda_1$ value is the difference in wavelength of the $S_0 \rightarrow S_2$ transition for PAAMeNp34 and PAAMeNp200. [c] The $\Delta\lambda_2$ is the difference between the wavelength maxima obtained from the fluorescence excitation spectra obtained at the monomer (320 nm) and excimer (440 nm) regions for PAAMeNp34.

Figure 1, a difference, between the spectra of the two polymers is seen at the red edge of the absorption band, whereas this difference is absent at more basic pH values (≥8.7). The band seen in the case of PAAMeNp34 at acidic pH values (not observed for the less-labeled PAAMeNp200 polymer), Figure 1, with maximum at ~340−350 nm should arise from additional ground-state absorbance of Np dimers. One additional observation resulting from a comparison between the data in Table 1 is the progressive decrease in the difference between the wavelength maximum (the $S_0 \rightarrow S_2$ transition) of the two polymers ($\Delta\lambda_1$) as the pH increases. At acidic pH values, this difference attains its maximum value and is close to ~1.6 nm (Table 1).

In addition, in Table 1, $\Delta\lambda_2$ is the difference between the wavelength maxima obtained from the fluorescence excitation spectra obtained at 320 and 440 nm for PAAMeNp34. (These do not coincide with the monomer and excimer emission maxima and were chosen to minimize the overlap of the monomer band in the excimer band and vice versa.)

Emission Spectra. The emission spectrum of the PAAMeNp34 polymer shows, at all pH values, the coexistence of the vibronically resolved monomer (with emission maxima at 320 nm) and the structureless excimer (with maxima at 390 nm) bands. In the case of the less-grafted naphthalene polymer, the excimer band is absent. This is illustrated, for the two polymers, at two different hydrogen ion concentrations, in Figures 2A and 2B.

At the monomer emission maximum (320 nm), there is little excimer emission; however, at the excimer emission maximum (390 nm), a significant amount of monomer emission can be observed. The overlap with the monomer emissive band is extensive for practically the entire emission region of the excimer, making it difficult to obtain the isolated excimer emission accurately. In the PAAMeNp34 case, the ratio of the excimer (I_E) to the monomer band (I_M), I_E/I_M, changes both with pH (Figure 2C) and the excitation wavelength (Figure 2D). An important observation made in Figure 2C is the increase in pH dependence of the I_E/I_M ratio at low pH values. When going from pH ≈ 3.3 to 3.8 (inflection point at ~3.4), the percentage of COOH groups ionized increases from ca. 3 to 10%. Note also that the chlorine ion seems to have a negligible quenching effect since pH adjustments made with HCl or with $HClO_4$ basically create the same curve shape (Figure 2C). Therefore, the increase at lower pH most likely results from the hydrogen bonding between the nondissociated COOH groups that may keep regions within the macromolecule in a more coiled conformational state. This special feature was also observed in a previous study made on the same polymer sample, where the interaction with surfactant was investigated.[4] At higher pH values, electrostatic repulsion between polymer units opens up the polymer chain, leading to a lower I_E/I_M ratio. In Figure 2D, the dependence of the excimer-to-monomer fluorescence intensity ratio on the excitation wavelength is shown. It can be seen that the I_E/I_M values are constant for wavelengths lower than 290 nm, but they increase sharply for longer excitation wavelengths due to ground-state dimers (GSD) absorption. Although the mentioned $S_0 \rightarrow S_1[^1L_b(^1B_{2u})]$ forbidden transition also contributes in the 290−310 nm region, it has practically no influence on the absorption spectra of the naphthalene chromophore since it possesses a very low absorption coefficient as mentioned above. As a consequence of this, it is in the longer wavelength region that the GSD-to-monomer relative absorption should be higher, which is reflected by the significant increase in the I_E/I_M ratio for excitation wavelengths above 290 nm.

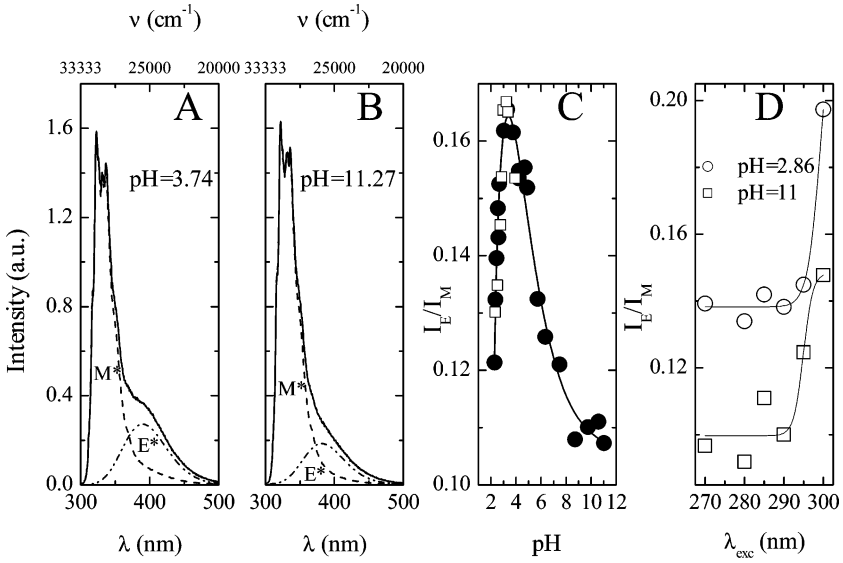

Figure 2. Fluorescence emission spectra of PAAMeNp34 (—) and PAAMeNp200 (- - -) at (A) pH = 3.74 and (B) pH = 11.27. (C) I_E/I_M ratio as a function of the pH (● obtained with HCl and □ obtained with perchloric acid) for the PAAMeNp34 system. (D) Dependence of the excimer-to-monomer fluorescence intensity ratio (I_E/I_M) on the excitation wavelength for PAAMeNp34 obtained at pH = 2.86 (○) and pH = 11 (□). The decomposed excimer band in parts A and B results from the spectral decomposition of PAAMeNp34 with PAAMeNp200 spectra. In the case of PAAMeNp200, the excimer band is absent. The excitation wavelength used in parts A−C was 281 nm. Parts C and D have associated errors (resulting from three independent experiments) of 5%. The size of the symbols used covers that error interval.

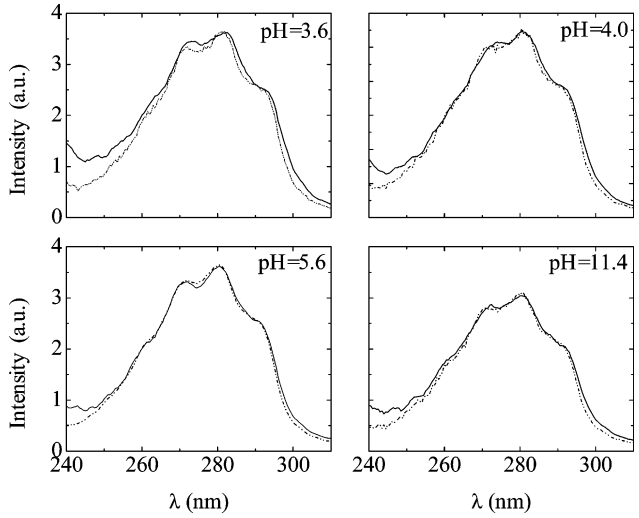

Figure 3. Fluorescence excitation spectra for PAAMeNp34 obtained at different pH values and collected at the monomer (320 nm, - - -) and excimer (440 nm, —) regions.

Excitation Spectra. Additional information concerning the kinds of interactions that exist within the polymer can be obtained from the fluorescence excitation spectra. Differences in these spectra, when collected in the monomer and excimer emission regions, are frequently used as evidence for ground-state dimers. This is particularly valid in the case of pyrene-based polymers, but it is also found in naphthalene-based polymers[4] although in a more tenuous way. In Figure 3, the fluorescence excitation spectra for PAAMeNp34 at different pH values and collected at two different wavelengths are shown.

It is quite obvious that a difference exists both in maxima and shape between the two spectra.[4] In particular, a broadening of the $S_0 \rightarrow S_1$ absorption band, which leads to a more pronounced absorption in the red and blue parts of the spectra can be seen when comparing the spectra collected at 320 nm (monomer emission band) and at 440 nm (excimer emission band). The 440 nm wavelength was chosen to minimize the monomer contribution at the excimer emission. This difference is more pronounced at acidic pH values. However, as shown in the excitation spectra, even at strongly basic pH there is evidence for a contribution from preformed dimers (Figures 2D and 3). In fact, for the PAAMeNp34 polymer, the observation of a displacement in the red edge of the naphthalene excitation spectra indicates the presence of ground-state dimers. As a consequence of this and of repulsive interactions that result from the presence of ionized carboxyl groups, which expand the polymer backbone, the total contribution for the excimer band will then mirror the balance of the hydrophobic interactions and electrostatic repulsions. For the former situation, this primarily results from the interaction of Np groups adjacent or in proximity along the chain. Regarding the latter situation, the ionization of the backbone structure will lead to a lower degree of hydrophobic association due to the more extended nature of the polymer. All of the above information results from a qualitative discussion, but additional parameters, extracted from the absorption and emission excitation spectra, can be used for a more quantitative line of argumentation and are summarized by the data in Table 1 for PAAMeNp34.

All of the differences in the absorption, emission, and excitation spectra and parameters related to them (Table 1) have their roots in the idea that a more or less intense absorption band, originating from ground-state aggregates, exists below the intense monomer band. With the gradual disappearance of the ground-state aggregates promoted by the increase in the pH or other external stimuli, for example, addition of surfactants,[4,5] all of the mentioned features tend to disappear.

Note that in the case of the $\Delta\lambda_1$ parameter, previously mentioned, there is a gradual decrease with increasing pH. This is a result of the lower degree of ground-state association at a higher pH in the PAAMeNp34 polymer case, i.e., a lower contribution of the dimer band below the intense monomer band. In the extreme situation, based on these data, one could expect that with PAAMeNp34 at basic pH values GSDs were totally absent, which is not entirely true. In fact, this parameter is not as sensitive as the parameters obtained from the steady-state fluorescence spectra and particularly the time-resolved fluorescence data (see below). In the case of the $\Delta\lambda_2$ parameter (Table 1), there is clear evidence for two different scenarios, one at acidic pH values and the other above pH = 6. In fact, the higher value for this parameter points to a larger contribution from GSDs at acidic relative to basic pH values.

In fact, if no GSD existed, i.e., if dynamic formation was the only route for excimer formation, then $\Delta\lambda_2 = 0$. Essentially, the variation in this parameter is more pronounced in the pyrene-based compounds from where data existing in the literature mainly comes.[3,5,10,29] However, in the present Np case, the fact that there is always a shift, independent of the pH value, between the excitation spectra collected at 320 and 440 nm ($\Delta\lambda_2 \neq 0$) points to the existence of excimer emission originating from ground-state dimers formed by Np groups that are in close proximity.[11] This is still valid at alkaline pH values, where the polymer is found in a more extended conformation.

Time-Resolved Fluorescence. Figure 4 shows the time-resolved decay profiles of a solution of PAAMeNp34 at pH = 4, obtained at two wavelengths and analyzed both with independent and global analysis. It can be seen that global analysis with two exponentials gives rise to fits with poor quality at both emission wavelengths (Figure 4A, see the weighted residuals, autocorrelation functions, and χ^2 values). When global analysis of the decays is made with three exponentials, the quality of the fits strongly increases (Figure 4B). However, the independent analysis of the decays leads to biexponential fits with only one common decay time (Figures 4C and 4D). In fact, at each wavelength, the independent analysis of the decays leads to biexponential decays in agreement with the data obtained by global analysis.

Independent analysis at the monomer emission wavelength (320 nm) yields fits with two or three exponential decays, depending on the weight of the competitive process of excimer dissociation. In the cases where this process is much slower than the excimer decay time τ_E, the component corresponding to this process in the decays is generally absent at 320 nm. Because of this, the decays follow biexponential laws (Figures 4B−D). This occurs, at room temperature, for pH values lower than 5.3 and above pH $\cong$ 7.3. Hence, in the range 5.3 < pH < 7.3, the a_{11} component (with a small value, Figure 5) needs to be considered, which would indicate some excimer-to-monomer reversibility to be operative. This is, however, in general, a nonsignificant deactivation pathway since this additional exponential is not needed to adjust all of the decays above pH = 5.5. Therefore, the subsequent determination of the excimer rate constant will be considered *without* the reversibility excimer-to-monomer (see discussion below).

As described above, in the case of the decays collected at the excimer region, when independent analysis is made, these will follow biexponential decay laws. Although it would be expected that some monomer emission contribution in the excimer region would lead to the presence of an additional decay

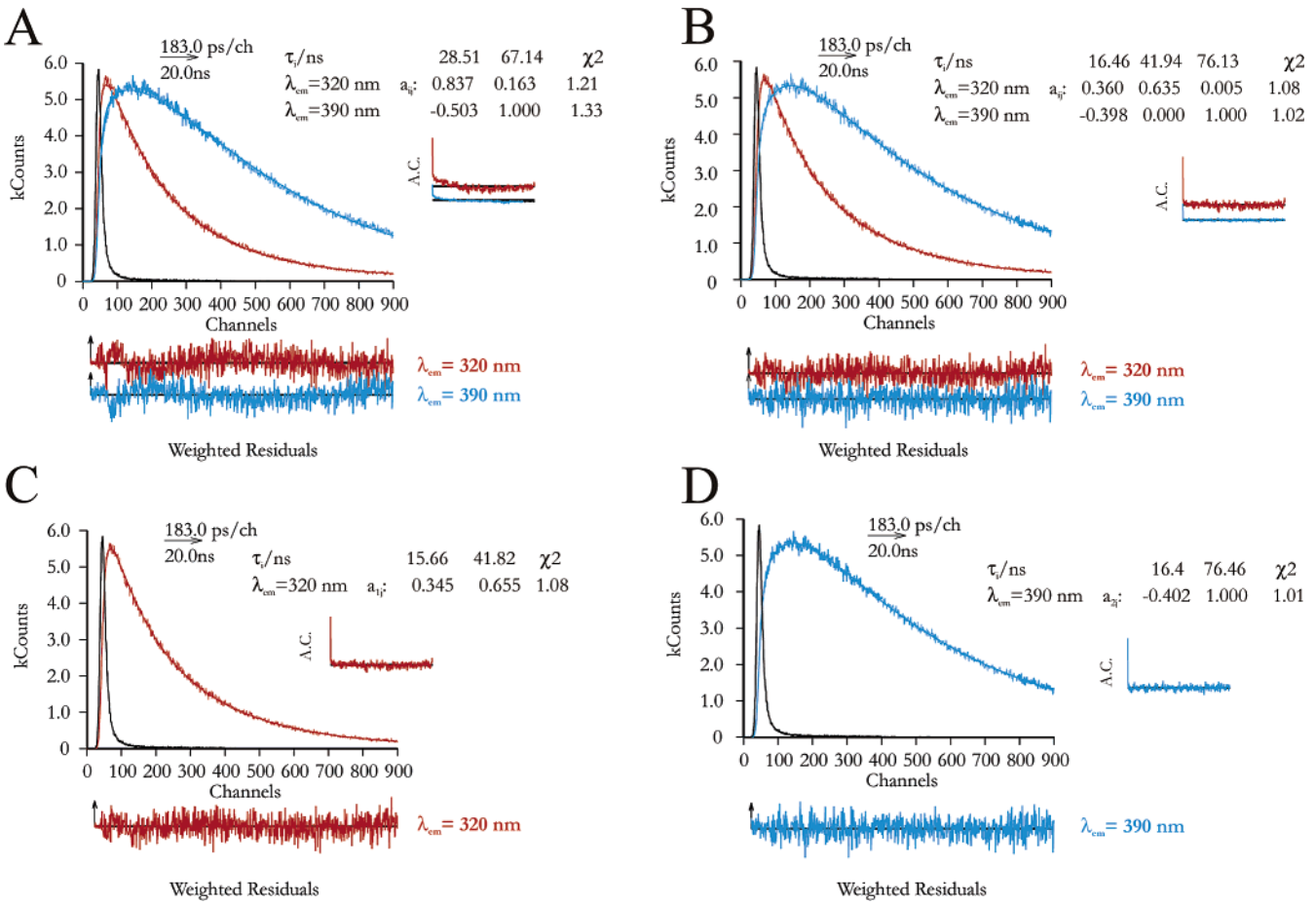

Figure 4. Fits of the fluorescence decays for PAAMeNp34 at pH = 4, obtained with global analysis of the decays with (A) a biexponential law, (B) a triple-exponential law and with independent analysis at (C) λ_{em} = 320 nm and (D) λ_{em} = 390 nm. Shown as insets are the decay times (τ in ns), preexponential factors (a_{ij}), and χ^2 values (χ^2) resulting from each analysis. Also shown are the autocorrelation functions (AC) and the weighted residuals for a better judgment of the quality of the fits.

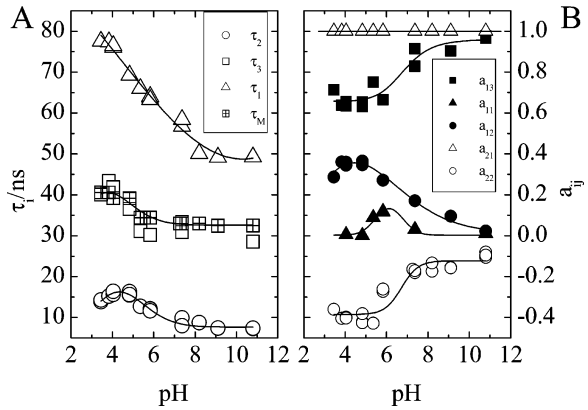

Figure 5. Variation of (A) the decay time values and (B) preexponential factors at 320 nm (a_{1j}) and 390 (a_{2j}) with pH for PAAMeNp34. Also shown is the fluorescence lifetime variation with pH for PAAMeNp200 (τ_M, ⊞). The lines shown are guidelines only. The data results from the best fit analysis to either independent or global analysis of the decays.

time, a third component does not seem to improve the quality of the fits. Even though the values of the three decay times seem to be well-separated, this could be due to some degree of mixing between two of the components, which will result in a mixed component. Alternatively, the absence of the third component (isolated monomer) may simply result because of the very low associated preexponential factor at $\lambda_{em} \geq 390$ nm.

In the case of intermolecular excimer formation for naphthalene and naphthalene derivatives, the literature reports the existence for Np of a monomer lifetime of 52 ns and an excimer lifetime of 380 ns in ethanol, whereas for 1-methylnaphthalene in the same solvent $\tau_M = 42$ ns and $\tau_E = 300$ ns are reported.[10] In a different solvent, such as toluene, values of $\tau_M = 110$ ns and $\tau_E = 80$ ns for Np and $\tau_M = 83$ ns and $\tau_E = 67$ ns for 1-methylnaphthalene are found in the literature.[10] These data reveal two important issues that are relevant to consider for future discussion of the present systems. First, they show that excimer lifetime can be longer or shorter than monomer lifetimes; this depends on the system and solvent. Second, it reveals that the naphthalene chromophores subjected to different substitutions display pronounced changes in their photophysical properties (its lifetimes in the illustrated example).

Figure 5 shows the pH dependence of the decay times and preexponential factors of PAAMeNp34 obtained at 320 nm (a_{1j}) and at 390−420 nm (a_{2j}), together with the fluorescence decay times of the less-labeled polymer, PAAMeNp200. The preexponential factors a_{13} and a_{12} reflect the concentration at time zero of two kinds of monomers, the isolated monomer and the monomer giving rise to excimer (MAGRE),[3] respectively. The preexponential a_{11} (which is practically zero at all pH values) reflects the weight of the reversible excimer dissociation process (Scheme 2). In the case of the preexponentials a_{22} and a_{21}, the former is associated with the decay time of the MAGRE monomer (and the formation time of the excimer negative preexponential), the latter with the excimer decay.[3] If only MAGRE forms excimer, the sum of a_{22} and a_{21} should be zero. A positive value implies that a large fraction of the excimer is

SCHEME 2

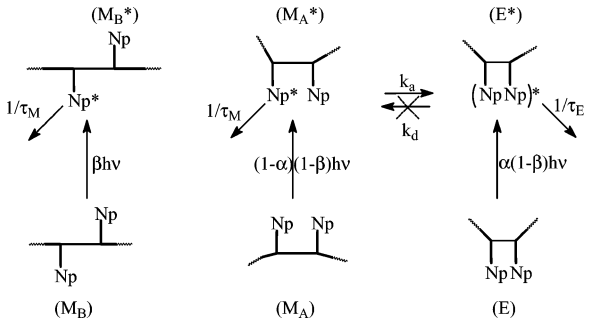

formed through direct excitation of preformed GSDs or that there is some emission "contamination" of the monomer decay in the excimer decay. This last situation was found to be unimportant at room temperature but relevant when time-resolved data is made as a function of temperature (see below). The present data results from the analysis of the decays with independent and global analysis as illustrated in Figure 4. One of the decay times (τ_3) is very close to the monomer lifetime (τ_M) of the less-labeled polymer (whose values are also shown for comparison). The observation that for PAAMeNp200 only the monomer emission band is present, together with the single-exponential nature of the decay, shows that, for the case of this polymer, the distance between neighboring Np chromophores within the PAA backbone is large enough to prevent excimer formation.[11] This means that only isolated Np chromophores are present with PAAMeNp200, and thus the results in Figure 5 suggest that in the case of the PAAMeNp34 polymer there are some isolated Np groups along the PAA chain, i.e., with no other neighboring Np.[11]

The simultaneous existence of dynamic excimer formation at basic pH values can be evaluated by the presence of a rise time (negative preexponential) associated with the shorter decay time, at the excimer emission wavelength, a_{22}. In general, it can be observed that all the decay times decrease with increasing pH until they reach their plateau values at pH $\approx$ 6−7 (Figure 5). The decrease is more pronounced for the longer decay time (associated with the excimer decay), and this is probably due to the more extended conformation adopted by the polymer, which may allow a more effective encounter between the fluorophores and the oxygen (quencher) molecules.[23] The values for the excimer lifetime are within the range (43−76 ns) found for polymeric systems with naphthalene excimer emission,[11,12,30,31] although reports of shorter decay times for excimer fluorescence exist in the literature for poly(naphthyl acrylate) and poly (naphthyl methacrylate), for different solvents and linking positions of the Np chromophore.[12,32,33] Also, with poly(ethylene terephthalate-*co*-2,6- naphthalene dicarboxylate) with different degrees of naphthalene, relatively short excimer fluorescence lifetimes, with values varying from 10.1 to 12.4 ns, have been reported.[34]

For the shorter decay time (τ_2), related to the MAGRE monomers, there is a progressive increase until pH $\cong$ 4 with a subsequent decrease followed by a plateau; see Figure 5. It is also worth noting that the preexponential factor associated with the isolated Np chromophores (a_{13}) increases with pH, whereas the a_{12} preexponential associated with the MAGRE monomers decreases with the pH from pH = 4. The balance between hydrophobic interactions leading to Np−Np association and repulsive electrostatic interactions resulting from the ionized carboxyl groups will, at higher pH, favor the latter leading to the existence of more isolated Np chromophores. As the pH increases, the negative preexponential (a_{22}) decreases in absolute value. This means that, globally, excimer formation (in this case dynamic contribution) loses importance as the pH increases. Again, this is in accordance with the findings regarding the increase in the number of isolated Np chromophores with the increase in the pH. The more extended the conformation the polymer adopts, due to the intraelectrostatic repulsions between the COO^- groups, the fewer Np groups are in the vicinity of each other. As a consequence, the excimer contribution (both static and dynamic) will be smaller in the emission spectra. However, since the polymer is randomly labeled, there will be locally an uneven population of Np segments. The more densely populated regions will be responsible for the remaining excimer observed in alkaline media.

Kinetic Analysis of Time-Resolved Fluorescence. As already shown, the present systems cannot be fit to a simple monomer−excimer (two-state model) Birks' kinetic scheme.[10] The validity of a Birks-type analysis of intramolecular excimer formation in polymers, where a single monomer should be found to be connected to one excimer, began to be questioned by the work of Phillips, Roberts, and Soutar[12,16,35] and by Holden and co-workers.[30] The need for a third exponential to properly fit polymer decays in the monomer region was then established for copolymers and naphthalene-containing polymers.[12,30] The need for a third exponential to properly fit the decays was also reported for the fluorescence decays of a naphthalene-containing polymer and attributed to a phosphorescent species.[34] Moreover, when ground-state dimers exist, the validity of Birks' kinetic scheme must be reexamined. In fact, when monomer-to-excimer formation is considered, the presence of ground-state dimers (GSDs) leads to a severe departure from the conventional kinetic formalism.

Different models and strategies to solve complex excited-state kinetics can be found in recent literature.[3,11,36−46] Among these, the so-called blob model has gained considerable recent attention because it yields quantitative results that agree with the qualitative information retrieved by other techniques (albeit these reflect different polymer concentration domains), allowing the validation of the obtained data.[38,46] As mentioned in the Introduction, within the blob model the fit to a law made of several exponentials will lead to a distribution of excimer formation rate constants, reflecting the existence of different chromophore microdomains on the polymer.[47] In an alternative approach,[3,11] which is partially similar to the one made in the present work, the rate constants for excimer formation are found with a single k_a, which nevertheless reflects some degree of distribution around that value but sharp enough to be fit with a mean value.

In the present work, all of the experimental data are consistent with the presence of two types of monomers and one excimer:[3,17,40] one isolated Np chromophore monomer (M_B), which is unable to participate in excimer (E*) formation, co-existing with the other type of monomer, M_A (MAGRE), which is able to form excimer during the lifetime of its excited state.

According to Scheme 2, the β value corresponds to the fraction of light that excites the isolated chromophores, M_B, while $1 - \beta$ is the light exciting the remaining chromophores (M_A and E) possessing one or more neighboring units. The fraction of light not absorbed by M_B can be further split in two components, $\alpha(1 - \beta)$, which is the fraction of light absorbed by ground-state dimers (E), and $(1 - \alpha)(1 - \beta)$, which corresponds to the fraction of light that directly excites the M_A monomers (MAGRE). The rates of excimer formation and dissociation are given by k_a and k_d, respectively. Also displayed in Scheme 2 are the reciprocals of the unquenched lifetimes of

the monomer and excimer, $1/\tau_M = k_M$ and $1/\tau_E = k_E$, i.e., the rate constants for monomer and excimer decay, both through radiative and nonradiative pathways.

According to Scheme 2, the time dependence of the excited-state concentration of each one of the species is given by

$$[M_B^*](t) = a_{13}\, e^{-\lambda_3 t} \quad (1)$$

$$[M_A^*](t) = a_{11}\, e^{-\lambda_1 t} + a_{12}\, e^{-\lambda_2 t} \quad (2)$$

$$[E^*](t) = a_{21}\, e^{-\lambda_1 t} + a_{22}\, e^{-\lambda_2 t} \quad (3)$$

where $\lambda_i = 1/\tau_i$.

Since at the monomer emission region both types of monomers contribute, the time dependence of monomer fluorescence can be described by the following equations

$$I_M(t) = I_{320nm}(t) = a_{11}\, e^{-\lambda_1 t} + a_{12}\, e^{-\lambda_2 t} + a_{13}\, e^{-\lambda_3 t} \quad (4)$$

and that of the excimer emission by

$$I_E(t) = I_{390-420nm}(t) = a_{21}\, e^{-\lambda_1 t} + a_{22}\, e^{-\lambda_2 t} \quad (5)$$

with λ_1 and λ_2 given by

$$2\lambda_{2,1} = (k_X + k_Y) \pm [(k_X - k_Y)^2 + 4k_a k_d]^{1/2} \quad (6)$$

where $k_X = k_a + 1/\tau_M$, $k_Y = k_d + 1/\tau_E$, and λ_3 is the reciprocal of the decay time of the uncoupled species. As described above, in general the monomer decays are fitted with the sums of two exponentials. Even in the cases where a third exponential is needed (some decays at pH values above 7 are sometimes better fit in the monomer region with three exponentials with the additional decay time identical to the one found at the excimer wavelength region), the associated preexponential (a_{11}) is always very small. Thus, it can be assumed that the time-dependent intensities in the monomer region (eq 4) can be reduced to biexponential laws for all pH values. As a consequence of this, eq 4 reduces to eq 7, and the limit of irreversibility ($k_E \gg k_d$) allows the association of the decay times to the species (see below).

$$I_M(t) = I_{320nm}(t) = a_{12}\, e^{-\lambda_2 t} + a_{13}\, e^{-\lambda_3 t} \quad (7)$$

As stated above, the back-reaction is insignificant at room temperature and at pH < 5.5 (and at pH > 7.3), i.e., $k_d \ll k_E$.

As previously seen,[3,11] the different decay times for PAAMeNp34 can be related to the species in Scheme 2. The decay time τ_3 is associated to isolated monomers since it presents a similar value to that found for PAAMeNp200, where excimer formation is not possible; the τ_1 and τ_2 decay times result from the overall processes in Scheme 2 and thus depend on the rate constants for the different processes. In the case of τ_2 and since the reversibility excimer-to-monomer can be neglected, $1/\tau_2$ is equal to the sum $k_M + k_a$ (see eq 8 below) and can consequently be associated to the MAGRE monomers. Similarly, $1/\tau_1$ and again in the view that there is nonreversibility excimer-to-monomer tends to k_E (the excimer decay rate constant). In fact, from eq 6 one can see that when $k_d = 0$, $\lambda_2 = k_X$, and $\lambda_1 = k_E$, i.e., the limiting solutions of this equation.

Under these conditions, the rate constant for excimer formation (k_a) can be obtained from the difference between the monomer decay time (τ_2) and the lifetime (τ_M) of the appropriate model compound not undergoing excimer formation (PAAMeNp200), eq 8. In this case, the τ_M value can also be considered to be identical to the τ_3 decay time, which is related to the lifetime of the isolated chromophores.[3]

$$k_a = \frac{1}{\tau_2} - \frac{1}{\tau_M} \quad (8)$$

In fact, it is interesting to note that τ_3 and τ_M in Figure 5A have approximately identical values. If this were not the case, i.e., if, for example, τ_3 were shorter than the τ_M values, then this would mean that during the lifetime of the isolated monomers they would become able to undergo dynamic excimer formation. As a consequence of the above and according to Scheme 2, the value of the preexponential factor a_{13} can be related to the β value. The α value can be obtained from the initial condition $a_{12} + a_{13} = 1 - \alpha(1 - \beta)$ together with simple manipulation of eq 7 leading to

$$\alpha = \frac{1 - (a_{12}/a_{13} + 1)a_{13}}{1 - a_{13}} \quad (9)$$

However, the rate constants obtained with eq 8 do not take into account the level of ground-state excimer association (related to α in Scheme 2). To obtain this value, a new relation must be derived[48] relating the excimer formation rate constants in the presence ($k_a(\alpha)$) and absence (k_a) of ground-state dimers

$$k_a(\alpha) = k_a - \alpha(k_a + k_M) \quad (10)$$

On the basis of this new $k_a(\alpha)$ value, a new k_X rate constant ($k_X(\alpha) = k_a(\alpha) + k_M$) can be calculated, and thus the excimer decay rate constant is now given by

$$k_E(\alpha) = \frac{1}{\tau_1} + \frac{1}{\tau_2} - k_X(\alpha) \quad (11)$$

The corresponding equations for all of the rate constants where the presence of the backward process is considered have been reported elsewhere for the analogous PAA polymer labeled with pyrene.[3] Equation 10 shows that the true rate constant has always a smaller value than the one obtained without considering the presence of ground-state dimers. This should be considered as an expected behavior since the existence of GSDs creates an additional nonactivated channel to excimer formation, which is responsible for an apparent decrease in the energetic barrier, leading to excimer formation in steady-state conditions, since both types of excimers (dynamic and static) will contribute to the observed excimer emission. In the view that the α values can be directly obtained through manipulation of the a_{1i} preexponential factors (eq 9), then $k_a(\alpha)$ and k_a can be obtained and compared. In Figure 6, the excimer formation ($k_a(\alpha)$ and k_a) and deactivation ($k_E(\alpha)$ and k_E) rate constants considering the presence and the absence of ground-state dimers are presented. It can be seen that the associative rate constants display identical behavior until pH $\cong$ 6. From there on, a significant difference is observed. Those rate constants that take into account the presence of ground-state dimers are always smaller than those with $\alpha = 0$, in accordance with eqs 10 and 11. Instead of considering the α value as directly obtained from the a_{1i} preexponential factors, this value could also be obtained from the sum of the preexponentials at the excimer wavelength, i.e., in conditions of nonreversibility, $a_{22} + a_{21} = \alpha$. However, due to the monomer emission contribution in the excimer region, this gives rise to higher α values.

The pronounced difference between the $k_a(\alpha)$ and k_a rate constants seems to reflect more the influence of the β parameter,

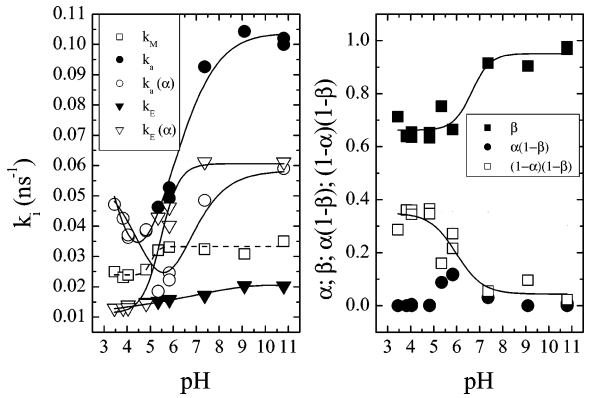

Figure 6. Variation with pH of (A) the association (k_a and $k_a(\alpha)$), excimer (k_E and $k_E(\alpha)$), and monomer decay (k_M) rate constants and (B) fractions exciting the M_A and M_B monomers (β and $(1-\alpha)(1-\beta)$) and the preformed excimers ($\alpha(1-\beta)$) at $T = 293$ K. The lines shown are guidelines only. Note that there is a practical overlap of the first four k_a and $k_a(\alpha)$ values (see text for more details).

due to its increase with pH, than that of the α parameter. The dependence of α and β on the pH can be directly monitored in Figure 6B. In fact, as can be observed in the figure, the β value increases with pH (from pH 6 to 7), whereas the fraction of light exciting the MAGRE (M_A) monomers ($(1-\alpha)(1-\beta)$) decreases and the fraction of light exciting the preassociated naphthalene ($\alpha(1-\beta)$) seems to decrease after pH 6. After pH $\approx$ 7.5, $\alpha(1-\beta)$ approaches zero, thus giving emphasis to the decrease in the total excimer formation. At this pH value, the polymer is negatively charged, and it must expand to accommodate the electrostatic repulsive forces existing between the ionized carboxyl groups. It is obvious that in this polymer extended conformation less naphthalene groups will be available to form excimers (both from static and dynamic routes), which is revealed both by the decrease in the steady-state excimer emission as well as by the increase in the a_{13} preexponential factor ($\equiv\beta$), since more "free" naphthalene groups will exist at high pH. Moreover, it is observed that the β value in Figure 6B levels out at alkaline pH values for a value of $\sim$0.93. Consequently, in this situation we expect to have, in this extended conformation, 93% of monomers nonneighboring and 7% of neighboring naphthalene monomers. Note also that there is a decrease in the τ_M lifetime (or increase in k_M), Figures 5 and 6, from pH $\approx$ 4 to pH $\approx$ 6, which again results from the change of the polymer PAA backbone from a coiled to a more expanded conformation.[49] This will result in that the naphthalene chromophores are more exposed to the aqueous environment in the latter case (alkaline pH values), which in turn will induce the possibility of additional quenching by oxygen. In acidic media, due to the coiled conformation of the polymer, the naphthalene chromophores are less exposed to the external environment. If the predominant way for excimer formation was the static route, which apparently is not the case as indicated by Figure 6B, then the preexponential factor a_{22} should have a positive value. It is observed in Figure 5 that the a_{22} preexponential possesses a negative value (rise time) up to pH = 11. Yet at these pH values, the excimer formation is dominated by the static route. This can be visualized by the strong decrease in the rise time (increase in absolute value of the a_{22} preexponential) and in the number of MAGRE monomers (reduced a_{12} preexponential in Figure 5), implying less dynamic excimer contribution. In the case of the a_{13} preexponential, Figures 5 and 6, the variation with pH exhibits a plateau from pH $\cong$ 3−6 with a subsequent increase until pH $\cong$ 8, then plateauing again, and thus resembles a typical titration curve. This is consistent with the increase in the number of isolated chromophores with pH as a consequence of the gradual change of the polymer chain from a coiled to a more expanded conformational state.[3] Since the nearby Np groups have strongly decreased in number, the total amount of excimer formation will be smaller.

A particular aspect revealed by Figures 2C, 5B (a_{12} preexponential factor), and 6 is also worth noting. For the parameters displayed in those figures, at acidic pH values (3.8−4.5), there is always an additional change of the parameter in consideration, in a general behavior that is to increase and then to decrease (Figures 2C and 5B) or the opposite (Figure 6A). This was previously observed for the I_E/I_M ratio as a function of the methanol content in methanol/water mixtures,[4,11] and it was interpreted in terms of a decrease in the extent of naphthalene aggregation with the increase in alcohol (good solvent) content in the polymer solution. However, with the analogous PAA labeled with pyrene this was not observed.[3] This seems to suggest that in the case of the PAAPy polymers a uniform and progressive opening of the coil structure of the polymer with pH occurs, which is reflected by the absence of a discontinuity in the I_E/I_M ratio.[3,5] On the contrary, the inflection point found for PAAMeNp34 (situated at pH $\cong$ 4.5−4.8) is consistent with the pK_a value reported for PAA in water (4.8)[50] and of one analogous PAAPy polymer (4.5).[22] This means that, in the present case, the level of dissociation of the carboxyl groups influences the photophysical behavior of the PAAMeNp34 polymer. Until the pK_a of the PAA is reached, association of the Np groups seems to prevail and to strongly aggregate the polymer. After the pK_a value is reached, the polymer progressively loses its coiled conformational nature, which is reflected in several photophysical parameters (Figures 2C, 5B, and 6). Here, we see an intriguing difference between PAA labeled with naphthalene and pyrene groups.[3,4,11] Albeit the reason behind this difference is not completely understood, we can give some further clues based on previous works of others on poly(methacrylic acid) (PMA) and PAA.[51,52]

The peculiar or anomalous shape of the plots of viscosity and apparent pK versus the degree of dissociation (α) for PMA was reported in the late 1960s by several authors.[51,52] The anomalies found were then explained as resulting from a cooperative conformational transition of the PMA polymer from a globular state to an expanded coil.[51,52] In those reports, the authors showed that the potentiometric plots of PMA revealed an anomaly at $\alpha \approx 0.15$, which was however absent in the titration curve of PAA.[52] Moreover, Crescenzi[52] reported that this effect was compatible with a transition from one type of PMA conformation (where the carboxyl groups were in an environment of low dielectric constant) to an open structure in which the ionized groups were allowed to become in contact with water. The nonexistence of this anomaly for PAA was explained on the basis of intramolecular interactions, absent or of lower importance for this polymer. In fact, for PMA in the region with a change from a dense coil to an expanded molecule, the van der Waals forces due to the methyl groups were considered to be important.[51] Therefore, the observed region was interpreted as an interval where a conformational transition between two different molecular forms of PMA would occur.[51] By analogy with the methyl groups in PMA (which is the only structural difference to PAA), we believe that the Np groups play a similar role, giving rise to a conformational transition between two conformational states of the PAAMeNp34 polymer. In fact, the weak van der Waals dimers (GSDs) that exist in greater proportion at acidic pH values gradually vanish with the increase in pH, giving rise to the expanded polymer, the

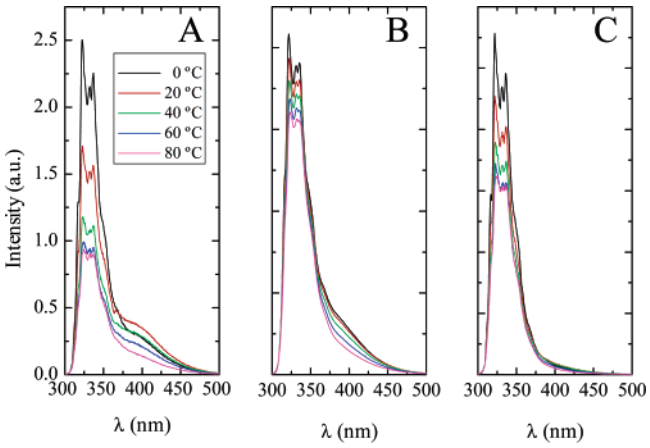

Figure 7. Fluorescence emission spectra as a function of temperature for PAAMeNp34 at (A) pH = 4, (B) pH = 11.4, and (C) for PAAMeNp200 at pH = 4. For all the experiments, the excitation wavelength was 281 nm.

total dimer contribution of which has decreased. Similar to the PMA case, there would be two distinguishable conformational molecular forms whose transition was gradual. However, why should we not observe this same pattern with the PAA polymer labeled with pyrene?[3] A possible answer to this may lie in the fact that the PAA labeled with pyrene will more easily form coiled structures (segment regions within the polymer) due to its more hydrophobic nature, and therefore the changes between the two conformations were now much more abrupt than with naphthalene as the hydrophobic chromophore.

Energetics

The fluorescence emission spectra at different temperatures of PAAMeNp34 in dilute water solutions at pH = 4 and 11.4 is shown in Figure 7 together with the spectra of PAAMeNp200 at pH = 4. The total fluorescence intensity decreases in all cases upon increasing the temperature without isoemissive points. For PAAMeNp34, the absence of isoemissive points indicates that monomer and/or excimer decay competes with the excited monomer (MAGRE)[22,53−55] (M_A^*) ↔ excimer (E*) direct and/or backward reactions and that the excited-state equilibrium is not reached before emission occurs. In the case of the PAAMeNp200 polymer, the decrease in intensity of the monomer band upon the increase in temperature is a consequence of the increase of the radiationless pathway relative to the radiative one.

***I*$_E$/*I*$_M$ Ratio.** The dependence of the photostationary fluorescence on temperature can nicely be rationalized by the so-called Stevens−Ban plots.[12,56] In these plots, the variation of the I_E/I_M ratio with the temperature, described within the framework of Birks' kinetic scheme, is given by eq 12[10,36,43]

$$\frac{I_E}{I_M} = \frac{k_F^E}{k_F^M}\frac{k_a}{k_d + k_E} \tag{12}$$

where $k_F^E = \phi_E/\tau_E$ and $k_F^M = \phi_M/\tau_M$ are the excimer and monomer radiative rate constants, which express the efficiency of excimer and monomer fluorescence, respectively. (ϕ_E and ϕ_M are the fluorescence quantum yields for the excimer and monomer forms.) The remaining rate constants have the meaning stated above. In general, when the temperature is increased, the excimer dissociation rate constant, k_d, increases faster than k_E, giving a limit where $k_d \gg k_E$ (high-temperature limit, HTL) and leading to a simplification of eq 12 to eq 13[36,43]

$$\frac{I_E}{I_M} = \frac{k_F^E}{k_F^M}\frac{k_a}{k_d} \tag{13}$$

This means that within this limit the ratio k_a/k_d reflects the equilibrium constant for the excimer formation. The opposite consideration, i.e., $k_d \ll k_E$ (low-temperature limit, LTL), leads to simplification of eq 1 to eq 14[36]

$$\frac{I_E}{I_M} = \frac{k_F^E}{k_F^M}\tau_E k_a \tag{14}$$

The resulting Arrhenius plots of $\ln(I_E/I_M)$ versus the reciprocal of the temperature, also known as Stevens−Ban plots,[56] will yield two straight lines, the slopes of which define, in the LTL, the activation energy for excimer formation (E_a)[36,43]

$$\frac{\mathrm{d}\ln\left(\frac{I_E}{I_M}\right)}{\mathrm{d}\left(\frac{1}{T}\right)} = -\frac{E_a}{R} \tag{15}$$

and, in the HTL, the enthalpy of formation (ΔH), or the binding energy, for the excimer complex[36]

$$\frac{\mathrm{d}\ln\left(\frac{I_E}{I_M}\right)}{\mathrm{d}\left(\frac{1}{T}\right)} = -\frac{(E_a - E_d)}{R} \tag{16}$$

The resulting Stevens−Ban plots[56] for PAAMeNp34 are presented in Figure 8. At low temperatures, the I_E/I_M ratio is small because excimer formation is restricted by the high viscosity of the solvent; this means that excimer formation is strongly restricted due to the difficulty of M_A^* and M_A species to diffuse. However, with the present system the proximity between nearby chromophores (resultant from the random labeling) can partially overcome this restriction. This partially results from the emission of the directly photoexcited GSDs, which may be stable at low temperatures.

Note that in Figure 8 the curves can be divided into two groups, those at acidic pH values (pH = 3.25 and pH = 3.82 i.e., below pH = 4) and those at basic pH values (above pH = 7.6). In the first group (acidic pH values), both regimes are clearly defined, whereas in the second group the LTL regime becomes ill defined, particularly at higher pH values. It is also clear that for lower pH values the parabolas are grouped differently than those at alkaline values. This means that the transition temperature between the LTL and HTL regimes (T^*),[10] inset in Figure 8, is found at 35−50 °C at acidic pH values, whereas for basic pH values this value is found around 15−20 °C (Table 2). This temperature transition depends not only on the nature of the formed excimer but also on solvent characteristics. The present study was concerned with water, and therefore the solvent characteristics can be considered to be a common factor for all of the obtained T^* values.

At acidic pH values, from the low-temperature limit regime and high-temperature limit regime, it is possible to extract the activation energy for the excimer formation, E_a, and the enthalpy of excimer formation (ΔH), calculated from the slopes in Figure 8. However, at basic pH values, the line defining the LTL is much more difficult to discern.

According to Scheme 2, the variation of the steady-state ratio of the excimer-to-monomer bands (I_E/I_M) can now be described[40]

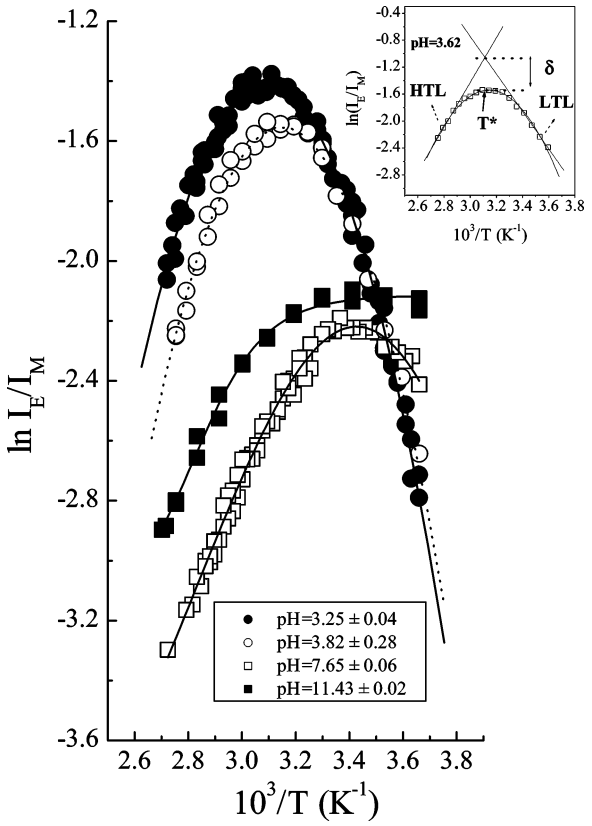

Figure 8. Plots of $\ln(I_E/I_M)$ vs $1/T$ obtained at different pH values for the PAAMeNp34 system. Shown as an inset is the parabolic-type curve with the HTL and LTL regions; the T^* and δ values are clearly identified.

by eq 17

$$\frac{I_E}{I_M} = \frac{k_F^E}{k_F^M} \frac{(\alpha k_M + k_a)(1-\beta)\tau_E}{\beta\tau_M k_a + k_d\tau_E + 1 - \alpha(1-\beta)} \qquad (17)$$

Equation 17 describes the temperature dependence of the I_E/I_M ratio since the included rate constants are functions of the temperature. Due to Scheme 2, the expressions for the HTL and LTL regimes are consequently also different, leading to, in the first case, where $k_d\tau_E \gg 1 - \alpha(1-\beta) + \beta k_a\tau_M$ (the HTL regime)

$$\left(\frac{I_E}{I_M}\right)_{HTL} = \frac{k_F^E}{k_F^M} \frac{(\alpha k_M + k_a)(1-\beta)}{k_d} \qquad (18)$$

In eq 18, it can be seen that the enthalpy of excimer formation, which is dependent on the k_a/k_d ratio, can no longer be retrieved due to the temperature-dependent term αk_M in the denominator of eq 18. The additional term $(1-\beta)$ is only slightly temperature-dependent and can therefore be considered constant as well as k_F^E and k_F^M. However, since the degree of aggregation decreases with temperature, the increase in temperature will eventually reduce the value of αk_M, and in the high-temperature limit, this term will vanish. As a consequence of this, the determination of ΔH will still be possible at high temperatures. The ΔH values retrieved from intermediate conditions should be considered as an upper limit since the temperature-dependent term $(1-\beta)$ in eq 18 will increase the value for the slope (in the HTL region) of the $\ln(I_E/I_M)$ versus $1/T$ plot.

When the LTL regime ($k_d\tau_E \ll 1 - \alpha(1-\beta) + \beta k_a\tau_M$) is considered, eq 17 reduces to

$$\left(\frac{I_E}{I_M}\right)_{LTL} = \frac{k_F^E}{k_F^M} \frac{\tau_E(\alpha k_M + k_a)(1-\beta)}{1 - \alpha(1-\beta) + \beta k_a\tau_M} \qquad (19)$$

In this situation, the presence of more than one temperature-dependent term (both in the numerator and denominator of eq 19) excludes the determination of the activation energy (E_a) associated with the excimer formation. In fact, this is reflected in the results at high pH values in the LTL region by a plateau (Figure 8, pH = 11.4), which expresses the domination of the aggregation-dependent term α (eq 19). This means that when practically all of the excimer-forming monomers are preassociated in the ground state, $\alpha \cong 1$, eq 19 becomes meaningless, and the ratio I_E/I_M is ruled by the ground-state dimers (Scheme 2). The decrease in the I_E/I_M ratio at low temperatures observed for high hydrogen ion concentrations, Figure 8 (contrasting the observed plateau at high pH values), reflects the decrease of the excimer formation rate constant, k_a, which in turn shows that the dynamic excimer contribution is important. Nevertheless, as shown from the time-resolved data, we have obtained negative preexponential factors even at high pH values (Figures 5 and 9). The reason for this is that, even in alkaline media, there is still some dynamic contribution to excimer formation.[11] One other possible explanation for the absence of the LTL limit at alkaline pH values resides in the fact that at these pH values, the dynamic contribution is due to monomers that are almost in excimer conformation (reflected in the increase of k_a with pH); since they form excimers with movements that involve short segments of the PAA chain, the activation energy is smaller, i.e, the excimer formation process is less activated, and consequently the LTL is not reached.

If we consider the distance between the intercept of the HTL and LTL regime lines and the normal regime (NR), the last being defined by the parabolic-type behavior found in the transition temperature, eqs 18 and 17 respectively, then the resulting δ value (defined in Figure 8) is given by eq 20

$$\delta_{HTL-NR} = \ln[2 - \alpha(1-\beta) + \beta k_a\tau_M] \qquad (20)$$

On the basis of this difference between the intercept of the limit lines and the NR regimes at the transition temperature (eq 20), we can separately consider the influence of isolated Np chromophores and of GSDs. In fact, if no isolated Np chro-

TABLE 2: Relevant Parameters Obtained from the Arrhenius Plots of $\ln(I_E/I_M)$ vs $1/T$ for PAAMeNp34 in Water at Four Selected pH Values[a]

pH	T^*[b] (°C)	δ[c]	$-\Delta H$[d] (kJ mol^{-1})	E_a^{ap}[e] (kJ mol^{-1})
3.3 ± 0.2	46 ± 2.5	0.62 ± 0.16	25 ± 5	27 ± 4
4.4 ± 0.5	37 ± 2.50	0.67 ± 0.14	25 ± 3	27 ± 4
7.62 ± 0.06	18 ± 2.22	0.64 ± 0.13	19 ± 1.4	
11.43 ± 0.02	*f*	0.89 ± 0.04	20 ± 0.8	

[a] The data results from the average of three to four independent experiments. [b] Transition temperature between the HTL and LTL regimes (T^*). [c] Difference (δ) between the curve defining the normal regime and the line defining the HTL regime at the crossing point, T^*, where $k_d = \tau_E$. [d] Enthalpy of excimer formation (ΔH). [e] Apparent activation energy (E_a^{ap}). [f] A plateau is reached, and therefore the transition temperature between the HTL and LTL is not possible to determine.

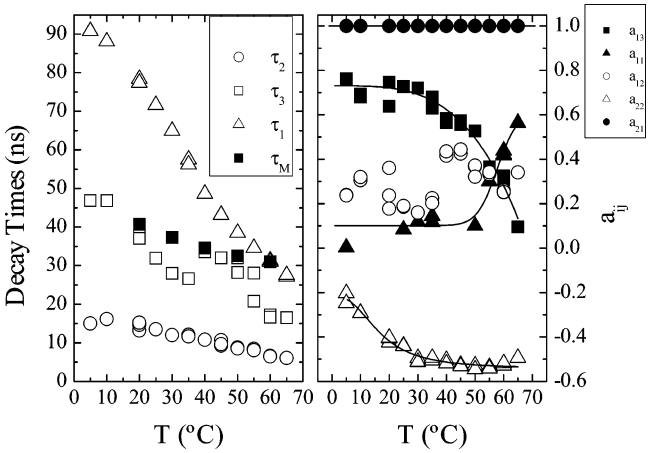

Figure 9. Temperature dependence of the decay times (τ_i) and preexponential factors (a_{ij}, i =1 at 320 nm and i = 2 at 390 nm) for PAAMeNp34 at pH = 3.8. Also shown is the variation of the fluorescence lifetime with temperature for PAAMeNp200 (τ_M) at the same pH value. The data results from the best fit analysis to either independent or global analysis of the decays.

mophores existed, i.e., if $\beta = 0$, then eq 20 would reduce to $\delta_{HTL-NR} = \ln [2 - \alpha]$, which means that the δ value under these conditions should always be smaller than ln 2 (0.693). Isolated chromophores are however, as previously shown from the time-resolved data, present at all pH values (Figure 5) and also at that temperature (crossover temperature between the HTL and LTL regimes $\cong$ 40−50 °C). If we now observe the values in Table 2, we can see that $\delta < 0.693$ for all pH values except the most alkaline. This means that the influence of GSDs for pH $\leq$ 11 is greater than that of isolated Np chromophores. With the increase in pH, the δ value increases as a consequence of the increase in the β value (eq 20). This establishes the fact that the influence of isolated chromophores increases with pH. Note also that this is in consonance of the time-resolved data where the preexponential factor a_{13} associated with β shows a corresponding behavior.[3]

Also of relevance is to notice that the ΔH and E_a values in Table 2 are not the true or intrinsic enthalpies and activation energies for excimer formation and should therefore be considered as apparent values (ΔH^{ap} and E_a^{ap}). In fact, these values are obtained from the slopes in the HTL and LTL regimes considering the absence of GSDs and isolated Np chromophores, i.e., from eqs 12−16; as a consequence, the enthalpy of excimer formation values can be estimated from the steady-state (HTL) data at any pH value. But since GSDs are present in the PAAMeNp34 system, the activation energy value for excimer formation can only be estimated at high hydrogen ion concentrations. Although the correct expressions for determining the intrinsic $\Delta H(\alpha)$ and $E_a(\alpha,\beta)$ are complex since they depend on all of the rate constants and also on the α and β values,[40] there are some further conclusions that can be made. The ΔH (or apparent enthalpy of excimer formation values, ΔH^{ap}) values seem to have, in acidic media, an average value of approximately −25 kJ/mol, whereas in alkaline media this value drops to approximately −20 kJ/mol. Even with an associated error of ±3 kJ/mol in the acidic region and ±1 kJ/mol in the alkaline region (Table 2), the values are clearly differentiated in these two regions. This is consistent with a less stable excimer with increasing pH as a consequence of an increase of the electrostatic repulsions induced by the carboxyl groups. (At pH values higher than 7, we know that 55% or more of the COOH groups are deprotonated.[4]) In the case of the activation energy values, in the situations where determination could be made (acidic region), they seem to present an identical value. The deduced intrinsic activation energy of excimer formation ($E_a(\alpha,\beta)$) now depends on the level of GSDs and isolated chromophores. In fact, the isolated chromophores do not participate in the excimer formation reaction and therefore should not be considered to affect the activation energy. In practical terms this means that, if no other factors are involved, $E_a(\alpha,\beta)$ can be reduced to $E_a(\alpha)$. However, the isolated chromophores fluoresce (all parameters are obtained through the I_E/I_M ratio, and I_M obviously includes emission of isolated chromophores), which consequently introduces some degree of error. The same is valid for the GSDs. In fact, what happens is that, as mentioned above, the slopes in the two regimes are associated with the thermodynamic parameters ΔH and E_a, when eqs 12−16 are used. When ground-state dimers and isolated chromophores are involved, with accompanying α and β factors, we cannot extract directly the enthalpy of excimer formation and the activation energy from the slopes of the Steven−Ban-like plots, and so the obtained parameters can only be considered to be apparent.[40] The intrinsic activation energy was found to be related to the apparent activation energy (E_a^{ap}), where no isolated chromophores are taken into account, through[40]

$$E_a(\alpha) = E_a^{ap} - \alpha E_e \tag{21}$$

where E_e stands for the dimer binding energy in the ground state.

Equation 21 shows that the intrinsic activation energy $E_a(\alpha)$ is lower than the apparent (E_a^{ap}). As α loses importance with increasing pH, i.e., less GSD contribution, then the $E_a(\alpha)$ value approaches the E_a^{ap} value. In the limit $\alpha = 0$, they will be identical. In the presence of isolated chromophores and absence of GSDs ($\alpha = 0$), the relation for the now true activation energy ($E_a(\beta)$) is given by[40]

$$E_a(\beta) = \beta k_a \tau_M E_a^{ap} \tag{22}$$

When only isolated chromophores are present, this β-dependent true activation energy ($E_a(\beta)$) is larger than the apparent one (E_a^{ap}). These two opposite trends of $E_a(\beta)$ and $E_a(\alpha)$ from eqs 21 and 22 are however compatible with the behavior observed; see Table 2. In fact, when the pH is increased, the number of isolated chromophores (i.e., the β value) increases, whereas the degree of ground-state association (related with the α value) decreases. From the photostationary dependence of the I_E/I_M ratio with temperature (Table 2), the two compensate the effect of each other, leading to a constant value for E_a^{ap}. However and again, values for E_a^{ap} were only able to be obtained in the acidic region, where data in the LTL regime exists (Figure 8 and Table 2). Nevertheless, it is important to realize, again, that the E_a^{ap} values in Table 2 are not the true values. However, as will be shown below, it is possible to extract the true activation energy values for excimer formation from time-resolved fluorescence data.

Time-Resolved Fluorescence. As shown above in the steady-state fluorescence data, both the low- and high-temperature regimes can be observed at acidic pH, whereas in alkaline media only the high-temperature regime is resolved. At acidic pH values, the transition temperature is found at 45−50 °C. In this case and in the studied temperature range 5−50 °C, the system is found in the LTL regime, which means that $k_E \gg k_d$, and consequently the rate constants k_a and k_E can be obtained, as shown previously (eq 8−10). Above pH $\cong$ 5.5, the system is in the low-temperature regime only up to ∼25−30 °C. This means that

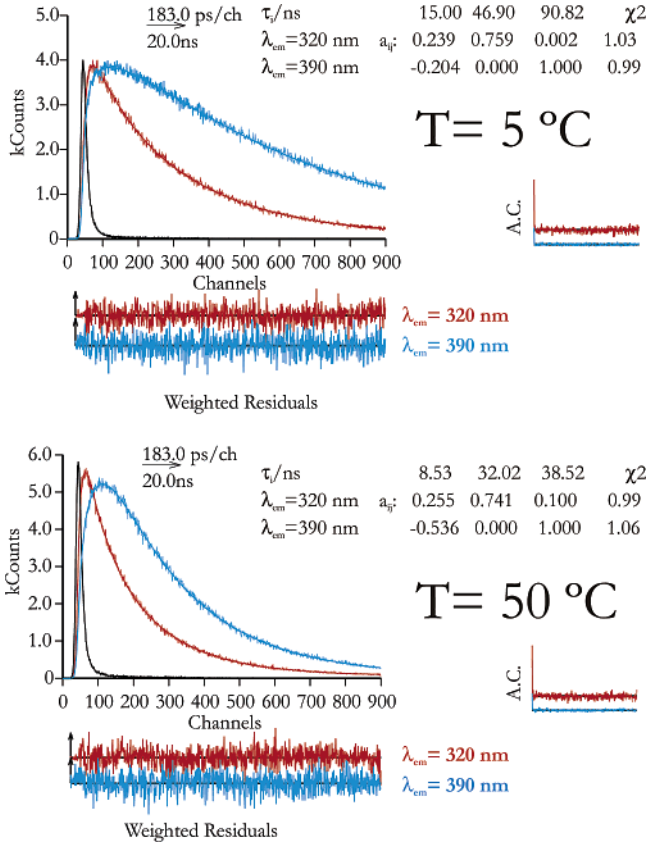

Figure 10. Fluorescence decays for PAAMeNp34 at pH = 3.83 and fits obtained with global analysis of the decays at 5 and 50 °C. Shown as insets are the decay times (τ in ns), preexponential factors (a_{ij}), and χ^2 values (χ^2). Also shown are autocorrelation functions (AC) and the weighted residuals for a better judgment of the quality of the fits.

within the mentioned temperature ranges, the temperature dependence of the time-resolved data can be treated, at all pH values, as a nonreversible system, i.e., no additional reverse excimer dissociation exists. As a consequence of this, the biexponential fluorescence decay that is observed in the monomer emission region corresponds to the decay of the MAGRE monomer (M_A^*) and of the isolated/free monomer (M_B^*).

The temperature dependence of the different decay times (τ_1, τ_2, and τ_3) for PAAMeNp34 and that of PAAMeNp200 (τ_M) is shown in Figure 9 for solutions at pH = 3.8. The general dependence consists of a decrease with temperature, thus showing that we are in the presence of an activated process (excimer formation). It can be seen that the temperature dependence of the fluorescence lifetime for PAAMeNp200 (τ_M) follows the same trend as that found for the decay time of the isolated chromophore (τ_3).

In addition, for these decay times (τ_3 and τ_M), the decrease with temperature is less significant than in the cases for τ_1 and τ_2. Also, the preexponential factor associated with the decay time τ_3 (a_{13}) displays a sharp decrease with the temperature. At λ_{em} = 390 nm, the preexponential factor associated with M_A^* (a_{22}) is negative (Figures 9 and 10). If no ground-state dimers were being excited or if no monomer emission was significant at this wavelength, then $a_{22} = -a_{21}$. But since this is not found, it means that either the GSD exists or a monomer emission is present. Since the major contribution to the monomer emission comes from the isolated (M_B^*) chromophores and there is no contribution from this monomer at λ_{em} = 390 nm, as seen from the absence of a third exponential at this wavelength (Figure 10), this means that the a_{22} preexponential has no contribution from the emission of M_B^* (and M_A^*) monomers at the 390 nm emission wavelength. As a consequence, the a_{22} preexponential factor shows that E* forms (in the excited state) at the expense of M_A^*, but it contains an additional contribution resulting from direct excitation of the GSDs (E in Scheme 2), i.e., $a_{22} = -a_{21} + f_1 A_{GSD}$ with f_1 dependent on the fraction of GSDs. Furthermore, as the temperature increases, a_{22} decreases. This fact, together with the concomitant decrease in the fraction of GSDs (reflected, for example, in the increase in absolute value of the negative preexponential, Figure 9), means that more dynamic excimers are being formed at the expense of more isolated Np chromophores. Hence, less free or isolated Np chromophores exist at elevated temperatures. At higher temperatures, there are more encounters between chromophores (which produce dynamic excimers) due to changes in polymer conformation. Note that in Figure 9 the preexponential a_{11} factor at the monomer emission wavelength associated with the excimer-to-monomer reversibility is low since the system is, between 5 and 50 °C, in the LTL regime. In fact, the a_{11} value ranges from 0.002 at 5 °C to 0.1 at 50 °C (Figures 9 and 10), increasing thereon since we than are entering the HTL (where $k_d \gg k_E$), and as a consequence, the reversible excimer-to-monomer process prevails over the excimer deactivation. The a_{11} value is never zero because at 320 nm there is some overlap of the excimer emission with the prevalent emission of the monomer. This can be clearly observed in Figure 2 where the spectral decomposition of PAAMeNp34 results in the monomer emission band with this last one with an ending tail at ~315 nm. With the current experiments, we have used 2-nm slits in the emission monochromator, which is equivalent to an effective wavelength bandpass of ca. 10 nm. The absence of the a_{11} preexponential (in fact, we can force the decay to have a third exponential, but no improvement in the quality of the decay fit is obtained, and the associated preexponential is residual) component at 20 °C in Figures 4 and 9 should therefore not be overemphasized and considered as merely a coincidence.

The temperature dependence of the rate constants extracted from the time-resolved fluorescence data at different pH values can be viewed through the Arrhenius plots that are presented in Figure 11.

Within the experimental error, all of the rate constants present linear trends, totally compatible with Arrhenius behavior. It is possible to observe that the rate constants obtained considering the presence of the GSDs (eqs 9 and 10) always have lower values than those obtained without considering the α parameter. From the slope of the plot of ln $k_a(\alpha)$ versus $1/T$, the true or intrinsic E_a values (denoted $E_a(\alpha)$) can be obtained; see Figure 11. It is worth noting that the determination of the activation energy values obtained from the slopes in Figure 11 ($E_a(\alpha,\beta)$ values) is not dependent on the level of isolated chromophores present, that is the β value. In fact, according to Scheme 2 and eq 9, it is only the rate constant for excimer formation that depends on the fraction of light exciting these monomers. In practical terms, it should be better defined as $E_a(\alpha)$ instead of $E_a(\alpha,\beta)$.

Emphasis should be put on the fact that the obtained values for the activation energies from the slopes in Figure 11 are those taking into consideration the presence of GSDs, i.e., the true or intrinsic E_a values. The comparison between the apparent E_a^{ap} values in Table 2 and those in Figure 11 shows that according to eq 21, the intrinsic activation energy value ($E_a(\alpha)$) always has a smaller value (~24 kJ/mol at pH = 3.07 and ~18.2 kJ/mol at pH = 4.02) than the apparent E_a^{ap} (~27 kJ/mol for pH = 3 and 4 in Table 2). For alkaline pH values, E_a^{ap} could not be determined (Table 2). Therefore, the decrease in activation ener-

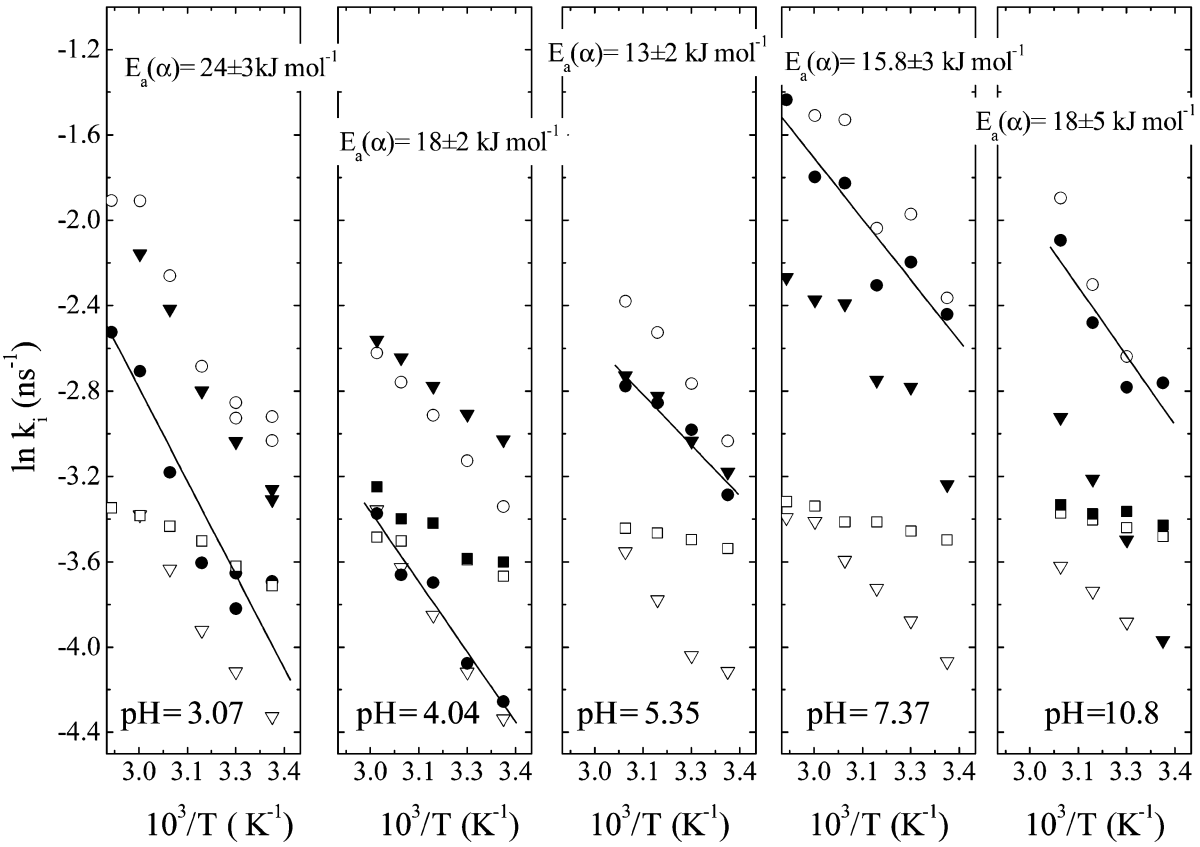

Figure 11. Arrhenius plots of the reciprocal temperature dependence of the logarithm of k_a (○), $k_a(\alpha)$ (●), k_E (▽), $k_E(\alpha)$ (▼), and of the reciprocal decay time of the isolated chromophore, $1/\tau_3$ (■).

gy (E_a^{ap}) with increasing pH (Figure 11) can be explained by the gradual decrease in importance of the α value and hence less GSD formation. As mentioned above, the low value for the activation energy at alkaline pH values is probably due to the fact that the dynamic excimer is being formed from nearby monomers (EFS), which involves the movement of short chain segments.

One important issue related to stability occurring in excimer-forming molecules is their binding energies (*B*). The binding energy of one excimer is simply the negative value of its enthalpy of formation, i.e., $B = -\Delta H$. Pyrene and perylene excimers have the highest binding energies, ca. 40 kJ/mol.[10,57] Relevant to the present study are naphthalene and 1-methylnaphthalene excimers, which have values of ca. 24 and 29 kJ/mol respectively.[10] It may be observed in Table 2 that the obtained values are, with the possible exception of those obtained at alkaline pH values, close to those found for naphthalene or substituted naphthalenes.[10] However, some precaution should be equated in this comparison since the data in the literature is for nonpolar solvents, whereas the present naphthalene systems were studied in water, and it is obvious that the solvent should play a (more or less) significant role.

Finally, we should compare the effect promoted by changing the hydrophobic group, and the percentage of it, included in the water-soluble polymer. Substitution of pyrene by naphthalene has been shown to induce a decrease in the hydrophobic association, which is manifested by the absence of excimer formation when the chromophore content is decreased (PAAMeNp200). In the case of the low labeled polymer, the concentration of naphthalene bound to the PAA polymer is apparently so low that no intrachain contacts between the Np groups are observed.[11] However, a lower level of pyrene, incorporated into the PAA polymer, still leads to excimer formation and therefore to intrachain contacts. This means that the hydrophobic force, induced by the hydrophobic group, is relevant to the coiled or expanded conformational nature acquired by the polymer. Therefore, PAA labeled with pyrene will lead more easily to coiled structures (segment regions within the polymer) due to the higher hydrophobic character of the fluorophore. Another relevant aspect is that the lifetime of pyrene is much longer than that of naphthalene, which facilitates the detection of more intramolecular associations in the less-labeled PAAMePy polymer system compared to those in the less-labeled PAAMeNp polymer system.

Summary and Conclusions

In the present work, different photophysical techniques (absorption, steady-state, and time-resolved fluorescence spectroscopies) were used to study the photophysical and solution behavior of a PAA polymer randomly labeled, with two levels of naphthalene, as a function of pH. Different degrees of Np labeling were found to lead to significantly different photophysical properties. With the less-labeled Np polymer, excimer formation was absent, whereas with the more highly labeled Np polymer excimer formation was found to occur at all pH values. The effect of ground-state aggregation was investigated. Rate constants for the processes of excimer formation and deactivation were obtained considering the presence and absence of ground-state dimers. It was shown that aggregation has the effect of decreasing the rate constants for excimer formation, dissociation, and deactivation. Isolated or free monomers were also found to be present at all pH values. The amount of these was found to increase with pH. Static and dynamic routes for excimer formation were found to coexist for the more highly labeled Np polymer. The data obtained from the steady-state excitation spectra are in agreement with dynamic fluorescence

data revealing that, although excimer formation through a static route is preferred at alkaline pH values, the dynamic route cannot be excluded in the view of the existence of a rise time at pH = 11. Two main reasons can be proposed for this. First, in alkaline media there is a strong increment of the isolated monomers since electrostatic repulsions resulting from the ionized carboxyl groups of the PAA skeleton preclude the movement of large segments of this polymer. Second, excimer formation occurs from two routes, GSD formation (which does not contribute to the activation energy) and from almost preformed (close to the EFS stage), which now leads to an increase in k_a value.

The temperature dependence of the steady-state fluorescence data (I_E/I_M ratio) allowed estimates (apparent values) of the activation energies and enthalpy for excimer formation, at different pH values. From the time-resolved data, the true or intrinsic activation energy was obtained. Comparison between the two reveals that the true or intrinsic activation energy is always smaller than the apparent activation energy. In both fluorescence techniques, the data disclose that at low temperatures, the GSD formation dominates in the system even at alkaline pH values, although the level of GSD formation is much higher at acidic pH values. As the temperature increases, the thermal movement of the polymer chain increases the possibility of dynamic excimer formation, and the GSD formation decreases both at acidic and alkaline pH values. It was also found that the amount of isolated chromophores that are not engaged in any kind of excimer formation decreases with increasing temperature and increases with increasing pH.

Acknowledgment. We thank Dan Anghel for providing the polymers. Financial support from the Portuguese Science Foundation (FCT) (J.S.S.M., B.L., and M.G.M.) and the Swedish Research Council (K.S.) is acknowledged. T.C. acknowledges the FCT for a Ph.D. grant (SFRH/BD/17852/2004). J.S.S.M. acknowledges Dr. J. C. Lima for a critical review of the manuscript and Professor J. M. G. Martinho (IST) for valuable comments and suggestions.

References and Notes

(1) Evans, D. F.; Wennerström, H. *The Colloidal Domain: Where Physics, Chemistry, Biology, and Technology Meet*, 2nd ed.; Wiley-VCH: New York, 1999.

(2) Jönsson, B.; Lindman, B.; Holmberg, K.; Kronberg, B. *Surfactants and Polymers in Aqueous Solution*, 2nd ed.; John Wiley & Sons: Chichester, 1998.

(3) Seixas de Melo, J.; Costa, T.; Miguel, M. G.; Lindman, B.; Schillén, K. *J. Phys. Chem. B* **2003**, *107*, 12605.

(4) Schillén, K.; Anghel, D. F.; Miguel, M. D.; Lindman, B. *Langmuir* **2000**, *16*, 10528.

(5) Anghel, D. F.; Toca-Herrera, J. L.; Winnik, F. M.; Rettig, W.; von Klitzing, R. *Langmuir* **2002**, *18*, 5600.

(6) Roberts, A. J.; Soutar, I. Luminescence of Macromolecules in Fluid Solution. In *Polymer Photophysics*; Phillips, D., Ed.; Chapman and Hall Ltd: London, 1985.

(7) Biddle, D.; Chapoy, L. L. *Polym. Photochem.* **1984**, *5*, 129.

(8) Skilton, P. F.; Ghiggino, K. P. *Polym. Photochem.* **1984**, *5*, 179.

(9) Drake, R. C.; Christensen, R. L.; Phillips, D. *Polym. Photochem.* **1984**, *5*, 141.

(10) Birks, J. B. *Photophysics of Aromatic Molecules*; Wiley: London, 1970.

(11) Costa, T.; Miguel, M. G.; Lindman, B.; Schillén, K.; Lima, J. C.; Seixas de Melo, J. *J. Phys. Chem. B* **2005**, *109*, 3243.

(12) *Polymer Photophysics*; Phillips, D., Ed.; Chapman and Hall Ltd: London, 1985.

(13) Holden, D. A.; Wang, P. Y. K.; Guillet, J. E. *Macromolecules* **1980**, *13*, 554.

(14) Sakai, H.; Itaya, A.; Masuhara, H.; Sasaki, K.; Kawata, S. *Chem. Phys. Lett.* **1993**, *208*, 283.

(15) Declercq, D.; Delbeke, P.; Deschryver, F. C.; Vanmeervelt, L.; Miller, R. D. *J. Am. Chem. Soc.* **1993**, *115*, 5702.

(16) Phillips, D.; Roberts, A. J.; Soutar, I. *J. Polym. Sci., Part B: Polym. Phys.* **1980**, *18*, 2401.

(17) Phillips, D.; Rumbles, G. *Polym. Photochem.* **1984**, *5*, 153.

(18) Lee, S.; Winnik, M. A. *Macromolecules* **1997**, *30*, 2633.

(19) Horta, A.; Pierola, I.; Macanita, A. Polymethylphenylsiloxane (Photophysics, Conformation, and Dynamics). In *Polymeric Materials Encyclopedia*; Salamone, J. C., Ed.; CRC Press: Boca Raton, FL, 1996; Vol. 8; p 6391.

(20) Vangani, V.; Duhamel, J.; Nemeth, S.; Jao, T. C. *Macromolecules* **1999**, *32*, 2845.

(21) Duhamel, J.; Kanagalingam, S.; O'Brien, T. J.; Ingratta, M. W. *J. Am. Chem. Soc.* **2003**, *125*, 12810.

(22) Anghel, D. F.; Alderson, V.; Winnik, F. M.; Mizusaki, M.; Morishima, Y. *Polymer* **1998**, *39*, 3035.

(23) Seixas de Melo, J. *Chem. Educ.* **2005**, *10*, 26.

(24) Anghel, D. F.; Saito, S.; Baran, A.; Iovescu, A. *Langmuir* **1998**, *14*, 5342.

(25) Seixas de Melo, J.; Fernandes, P. F. *J. Mol. Struct.* **2001**, *565*, 69.

(26) Seixas de Melo, J.; Silva, L. M.; Kuroda, M. *J. Chem. Phys.* **2001**, *115*, 5625.

(27) Stricker, G.; Subramaniam, V.; Seidel, C. A. M.; Volkmer, A. *J. Phys. Chem. B* **1999**, *103*, 8612.

(28) Malkin, J. *Photophysical and Photochemical Properties of Aromatic Compounds*; CRC Press: Boca Raton, FL, 1992.

(29) Winnik, F. M. *Chem. Rev.* **1993**, *93*, 587.

(30) Holden, D. A.; Wang, P. Y. K.; Guillet, J. E. *Macromolecules* **1980**, *13*, 295.

(31) Coulter, D. R.; Liang, R. H.; Distefano, S.; Moacanin, J.; Gupta, A. *Chem. Phys. Lett.* **1982**, *87*, 594.

(32) Aspler, J. S.; Guillet, J. E. *Macromolecules* **1979**, *12*, 1082.

(33) Merleaubry, L.; Holden, D. A.; Merle, Y.; Guillet, J. E. *Macromolecules* **1980**, *13*, 1138.

(34) Jones, A. S.; Dickson, T. J.; Wilson, B. E.; Duhamel, J. *Macromolecules* **1999**, *32*, 2956.

(35) Phillips, D.; Roberts, A. J.; Soutar, I. *J. Polym. Sci., Part C: Polym. Lett.* **1980**, *18*, 123.

(36) Seixas de Melo, J.; Pina, J.; Pina, F.; Lodeiro, C.; Parola, A. J.; Lima, J. C.; Albelda, M. T.; Clares, M. P.; Garcia-Espana, E.; Soriano, C. *J. Phys. Chem. A* **2003**, *107*, 11307.

(37) Kanagalingam, S.; Ngan, C. F.; Duhamel, J. *Macromolecules* **2002**, *35*, 8560.

(38) Kanagalingam, S.; Spartalis, J.; Cao, T. M.; Duhamel, J. *Macromolecules* **2002**, *35*, 8571.

(39) Dias, F. B.; Lima, J. C.; Pierola, I. F.; Horta, A.; Macanita, A. L. *J. Phys. Chem. A* **2001**, *105*, 10286.

(40) Macanita, A. L.; Horta, A.; Pierola, I. F. *Macromolecules* **1994**, *27*, 3797.

(41) Macanita, A. L.; Horta, A.; Pierola, I. F. *Macromolecules* **1994**, *27*, 958.

(42) Seixas de Melo, J.; Macanita, A. L. *Chem. Phys. Lett.* **1993**, *204*, 556.

(43) Seixas de Melo, J.; Albelda, M. T.; Diaz, P.; Garcia-Espana, E.; Lodeiro, C.; Alves, S.; Lima, J. C.; Pina, F.; Soriano, C. *J. Chem. Soc., Perkin Trans. 2* **2002**, 991.

(44) Albelda, M. T.; Garcia-Espana, E.; Gil, L.; Lima, J. C.; Lodeiro, C.; Seixas de Melo, J.; Melo, M. J.; Parola, A. J.; Pina, F.; Soriano, C. *J. Phys. Chem. B* **2003**, *107*, 6573.

(45) Dias, F. B.; Macanita, A.; Seixas de Melo, J.; Burrows, H. D.; Güntner, R.; Scherf, U.; Monkman, A. P. *J. Chem. Phys.* **2003**, *118*, 7119.

(46) Picarra, S.; Relogio, P.; Afonso, C. A. M.; Martinho, J. M. G.; Farinha, J. P. S. *Macromolecules* **2003**, *36*, 8119.

(47) Picarra, S.; Duhamel, J.; Fedorov, A.; Martinho, J. M. G. *J. Phys. Chem. B* **2004**, *108*, 12009.

(48) Zachariasse, K. A.; Macanita, A. L.; Kuhnle, W. *J. Phys. Chem. B* **1999**, *103*, 9356.

(49) Mori, H.; Seng, D. C.; Lechner, H.; Zhang, M. F.; Muller, A. H. E. *Macromolecules* **2002**, *35*, 9270.

(50) Mandel, M. *Eur. Polym. J.* **1970**, *6*, 807.

(51) Leyte, J. C.; Mandel, M. *J. Polym. Sci., Part A: Polym. Chem.* **1964**, *2*, 1879.

(52) Crescenzi, V. *Adv. Polym. Sci.* **1968**, *5*, 358.

(53) Turro, N. J.; Arora, K. S. *Polymer* **1986**, *27*, 783.

(54) Arora, K. S.; Turro, N. J. *J. Polym. Sci., Part B: Polym. Phys.* **1987**, *25*, 243.

(55) Arora, K.; Turro, N. J. *J. Polym. Sci., Part A: Polym. Chem.* **1987**, *25*, 259.

(56) Stevens, B.; Ban, M. I. *Trans. Faraday Soc.* **1964**, *60*, 1515.

(57) Katoh, R.; Sinha, S.; Murata, S.; Tachiya, M. *J. Photochem. Photobiol., A* **2001**, *145*, 23.